

Simulation of Particle Behavior in Charging Process of Blast Furnace by Discrete Element Method

Hiroshi MIO*

Yoichi NARITA

Abstract

This paper describes the development of a particle flow simulator for optimizing the charging process of a blast furnace by using Discrete Element Method (DEM). The particle behaviors during charging and discharging for a surge hopper or a parallel hopper were simulated. The large particles remained near the side wall of the hopper due to the particle size segregation during flowing on the heap. These particles tend to be discharged last when they are discharged from the hopper. Thus, it is found that the mean particle size of discharged particles increases with the increase in time.

1. Introduction

A blast furnace is a countercurrent moving-bed gas-solid reactor in which iron ores are reduced to produce pig iron. Ores (e.g., sinter and pellets) and coke are charged in layers by stacking them alternatively from the throat and hot gas is blown in from the tuyere at the lower section of the furnace. The permeability of gas in a furnace is a very important factor in the operation of the blast furnace. Keeping the gas flow stable is essential to stabilize the operation of a blast furnace and enhance its efficiency. Therefore, it is necessary to understand the behavior of ores and coke charged into a furnace, particle segregation, locations at which they build up, and the quantity ratio to render the burden distribution appropriate.

However, sinter, coke, and other types of granular materials charged into a blast furnace behave peculiarly; during flowing, certain types of particles gather in an unbalanced way in terms of space and time due to the difference of properties (e.g., particle size, density, surface properties, and particle shape) between particles. This phenomenon is called "segregation." Consequently, particles of a certain size and some brands gather concentratedly in the storage tank (e.g., hopper) provided in the course of transportation to a blast furnace and during charging into the furnace. Therefore, new techniques for predicting such particle behavior and segregation accurately and for controlling such behavior are highly desired, where particle simulation using Discrete Element Method (DEM)¹⁾ is gaining attention.

DEM, a simulation method proposed by Cundall et al. in the 1970s, analyzes the behavior of an entire particle group by turning all forces working on the particles (e.g., contact force, Coulomb

force, adhesion force, magnetic force, and drag force) into a model and solving equations of motion for individual particles one by one. DEM can analyze the behavior of particulates accurately because the method handles particles as discrete elements. Many researchers around the world have been working on it (e.g., mixing, crushing, powder transfer, filling, fluidized beds, and electrophotography).²⁻¹⁰⁾ Some have reported analysis examples for the processes related to blast furnaces¹¹⁻¹⁷⁾ and further advancement in the future is expected. The authors have been developing a method to simulate the burden distribution of a blast furnace using DEM for approximately ten years.¹⁸⁻²³⁾ This paper introduces examples of analysis of the influence of particle segregation in the transfer process to a blast furnace.²¹⁾

2. Discrete Element Method

The basic algorithm of DEM is to turn all forces working on particles into a model and to solve equations of translational motion and rotary motion for each particle in a discrete time period one by one.

$$\dot{\mathbf{v}} = \frac{\sum \mathbf{F}}{m} \quad (1)$$

$$\dot{\boldsymbol{\omega}} = \frac{\sum \mathbf{M}}{I} \quad (2)$$

Where, \mathbf{v} is the velocity of the particle, $\boldsymbol{\omega}$ is its angular velocity, \mathbf{F} is the force working on the particle, \mathbf{M} is the moment, m is the mass of the particle, and I is the moment of inertia. In particle behavior analysis in the charging process for a blast furnace, only the contact

* Senior Researcher, Dr. (Eng.), Ironmaking Research Lab., Process Research Laboratories
20-1 Shintomi, Futtsu City, Chiba Pref. 293-8511

force when particles come into contact and the gravity need to be considered as the working force (\mathbf{F}). In other processes involving particulates, various phenomena can be analyzed by considering fluid drag, magnetic force, electrostatic force, adhesion force, and other force types.

Regarding the collision between particles or between a particle and structure, the plastic deformation of the particles and damage to them are not taken into account and local overlapping is accepted. Therefore, when the formula below holds good, it is determined that the two particles have collided.

$$d < r_i + r_j \quad (3)$$

Where, d is the distance between the centers of the two particles, r is the radius of the particle, and i and j are particle numbers. In addition, the particle collision model is not that of perfectly elastic collision and it is a Voigt model consisting of a spring and dash pot shown in Fig. 1. The particle's elastic and non-elastic properties are expressed by an elastic spring (elastic constant: K) and a viscous dash pot (viscosity constant: η) inserted between the contact points.

In addition, to express friction that accompanies the collision of particles, a frictional slider (coefficient of friction: μ) was inserted in the shear direction. The force working on the contact area of the particles in the normal direction (\mathbf{F}_n) can be calculated with formula (4) below and the force in the shear direction (\mathbf{F}_t) can be calculated with formula (5).

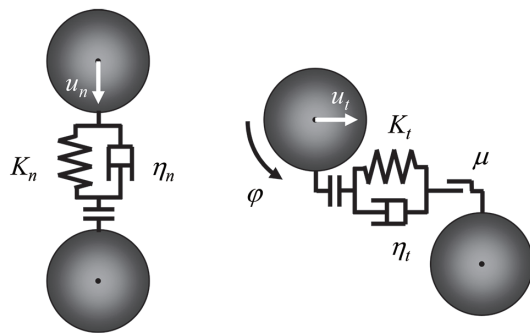
$$\mathbf{F}_{n,ij} = \left(K_n \Delta u_{n,ij} + \eta_n \frac{\Delta u_{n,ij}}{\Delta t} \right) \mathbf{n}_{ij} \quad (4)$$

$$\mathbf{F}_{t,ij} = \min \left\{ \mu \left| \mathbf{F}_{n,ij} \right| \mathbf{t}_{ij}, \left[K_t \left(\Delta u_{t,ij} + \Delta \varphi_{ij} \right) + \eta_t \left(\frac{\Delta u_{t,ij} + \Delta \varphi_{ij}}{\Delta t} \right) \right] \mathbf{t}_{ij} \right\} \quad (5)$$

Where, u is the relative displacement of the two particles at the contact point due to translation, φ is that due to rotation, \mathbf{n} is the unit vector in the normal direction, and \mathbf{t} is that in the shear direction.

The contact force and moment between the i -th particle and each of all the particles that are in contact with the i -th particle are calculated and added; the translation and angular velocity is calculated; and the displacement of the i -th particle from time t to $t + \Delta t$ is calculated. These calculations are repeated for all the particles until t becomes t_{\max} , which allows the behavior of the entire particle group to be simulated.

Usually, particles are regarded as globes in DEM, but the shape of most of the particles to be analyzed is not spherical. Therefore, resistance is often applied to the rotary motion of particles to consider their shape. In this study, rolling friction (moment) shown as the formula below was applied to the particles.



(a) Compressive force (b) Shear force
Fig. 1 Model for contact force

$$\mathbf{M}_{r,i} = -\frac{3}{8} \alpha_i b \left| \mathbf{F}_n \right| \frac{\boldsymbol{\omega}_i}{|\boldsymbol{\omega}_i|} \quad (6)$$

Where, b is the radius of the contact area and α is the coefficient of rolling friction. The shape of sinter and coke particles handled in this study cannot be the same. Therefore, our model in DEM was configured such that all the particles had a different coefficient of rolling friction (α) to allow individual particles to roll differently from the others. The distribution of α was determined based on the past study¹⁸⁾ in which one particle was dropped onto a slanted flat plate to calculate the distribution of rolling distances and its trend was compared with the behavior of the particle when it flew into the chute.

3. Simulation Conditions

Our study used DEM to simulate charging into and discharging from a surge hopper and a parallel hopper provided over the throat in the charging process for a blast furnace shown in Fig. 2. Test equipment that was a hopper scaled down to one third the size of an actual furnace was turned into a model, so the size of sinter particles was determined as 10.5 to 20 mm in diameter and the transportation quantity was 5.5 tons. Table 1 lists the number of particles for each size. The total number of particles is 1 262 876. The height of the surge hopper is approximately 3 m and the width is approximately 1.5 m. Sinter was charged from the conveyor belt installed over the hopper at a mass velocity of 23.4 kg/s.

As determined conditions, it was assumed that sinter on the conveyor belt had been completely mixed and no segregation was seen in terms of time and space. The height of the cylindrical parallel hopper is approximately 3 m and the diameter is approximately 2 m. Sinter was charged into one of the two hoppers from the conveyor

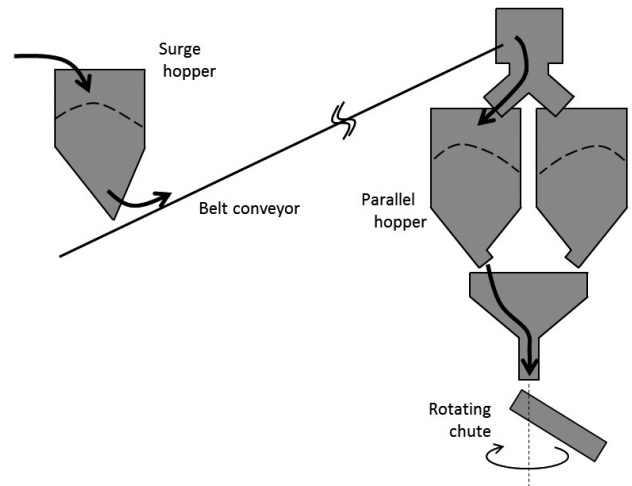


Fig. 2 Schematic illustration of charging process of blast furnace

Table 1 Particle conditions for simulation

Diameter [mm]	Number of particles [-]
10.5	549 936
12.5	325 949
15	188 628
17.5	118 786
20	79 577

belt over the throat via the switching chute. In the simulation, Δt was determined as $1.75 \mu s$ and sinter was charged into the surge hopper for 250 seconds and into the parallel hoppers for 110 seconds. After the sinter was charged into the hopper and all particles completely settled down, the hopper gate in the lower section was opened to simulate the discharge behavior and to study particle segregation during charging and discharging. All the calculations were made by the shared memory type parallel computation using OpenMP.

4. Results and Consideration

Figure 3 shows the behavior when sinter was charged into the surge hopper. The particles in the figure are classified by color based on their size: 10.5-mm particles in sky blue, 12.5 mm in pink, 15 mm in yellow, 17.5 mm in green, and 20 mm in red. The figure shows that as the charging proceeds, the sedimentary layer in the hopper becomes higher and many coarse particles (red) remain on the sedimentary slope and near the hopper wall. This is because coarse particles flew in below the slope due to particle segregation when they flew onto the slope. **Figure 4** is a contour map of mean particle size in the sedimentary layer after the charge into the hopper. The three figures are the cross sections of the hopper: Fig. 4(a) shows the vertical cross section at the center (relative position: 0.5), 4(b) shows the vertical cross section near the wall (relative position: 0.9), and 4(c) shows the horizontal cross section. The cross section at the center shows that mainly particles around the mean size of the charged particles are distributed around the center zone (charge point): It also shows that particles in the middle of the slope have a smaller diameter and particles near the wall have a larger diameter.

The horizontal cross-sectional view also shows this trend clearly. The figure shows that the mean size of the particles near the hopper wall is very large. This phenomenon is particle size segregation commonly seen when particles flow. In addition, Fig. 4(b) shows slight striped patterns in parallel to the sedimentary slope. This is

because when particles build up, the slope grows until its angle reaches the particles' angle of repose and it collapses at a stroke once the angle becomes larger than it. This periodic collapse affects the influx and segregation of particles, which produces striped patterns as seen in the figure. This is a phenomenon peculiar to particulates and it can be said that DEM can reproduce this phenomenon properly.

Figure 5 shows discharge behavior from the surge hopper. The

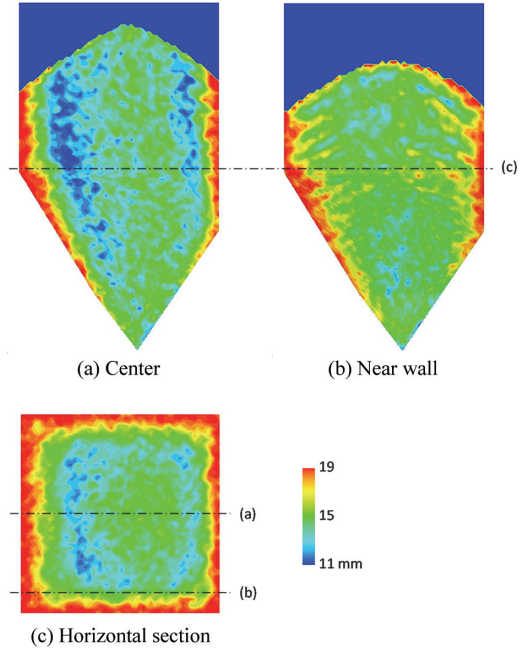


Fig. 4 Contour mapping of mean particle size of charged particle in the surge hopper

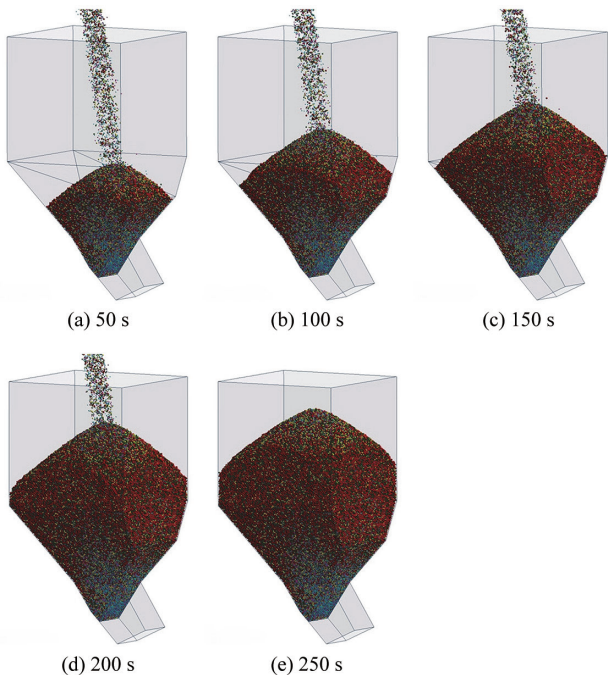


Fig. 3 Snapshots of particle behavior during charging into the surge hopper

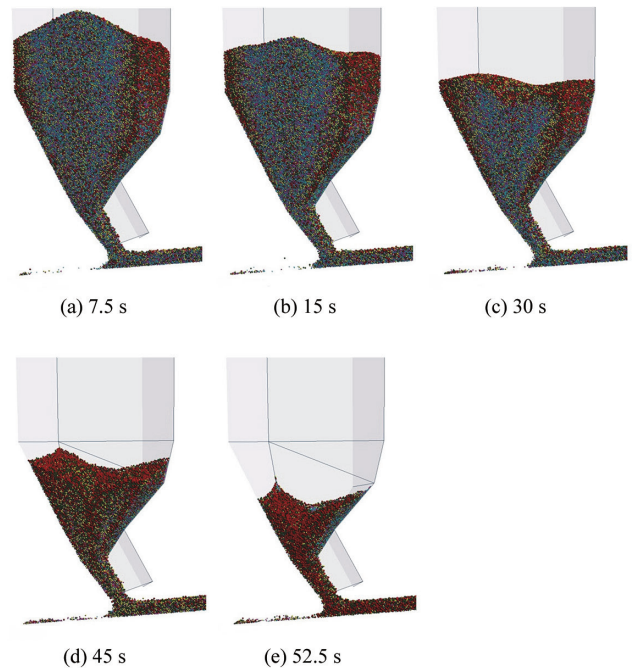


Fig. 5 Snapshots of particle behavior during discharging from the surge hopper

figure shows the cross section of the center (cross section the same as that in Fig. 4(a)). This figure shows that as the time passes, the center sinks and thereby discharge of particles near the wall lags. In addition, in the early phase of the discharge, many fine particles (sky blue) exist near the center of the cross section, but the number gradually decreases and in the last phase of the discharge, most remaining particles are coarse. **Figure 6** shows time changes in the normalized discharged mass of fine particles (10.5 mm) and coarse particles (20 mm). The graph shows that most of the fine particles are discharged by the middle phase and, on the contrary, the number of coarse particles abruptly increases as the discharge proceeds toward the end. This is possibly due to the influence of the relation between particle size distribution in the hopper and the order of discharge from the hopper shown in Fig. 4, and particle size segregation in the discharge movement.

Figure 7 is a map showing the order of discharge from the hopper. All particles in the hopper are classified by color based on their discharge timing (by one-tenth of the total discharge time). They are discharged in the order of red, green, yellow, pink, gray, blue, orange, greenish-yellow, brown, and sky blue. The map shows that the particles are discharged from the hopper outlet concentrically and ovally, and particles near the wall are discharged at a much slower pace. As shown in Fig. 7(b) and 7(c), the particles at the corners of the hopper are left to the very end. Many coarse particles build up at these zones due to segregation at the time of charging as shown in Fig. 4, indicating that many coarse particles are left to the latter period of the discharge from the hopper.

The sinter discharged from the surge hopper is charged into the parallel hopper over the throat via the conveyor belt for charging. **Figure 8** shows the charging behavior simulated by DEM (in 80 seconds). The figure visually shows that when particles build up in the parallel hopper, they segregate as is the case with the surge hopper and that many coarse particles gather near the wall. **Figure 9** is a contour map showing mean particle size distribution in the sedimentary layer. Figure 9(a) showing the vertical cross section at the center shows that the trend is slightly different from that in Fig. 4, indicating that the mean particle size on one slope is markedly big-

ger than that on the opposite slope. This is due to the influence of the movement in the switching chute before particles are charged into the parallel hopper. As shown in **Fig. 10**, when particles flow into the chute, fine particles segregate in the lower layer of the flow and particles are emitted from the chute in such segregated state, so more fine particles gather on the right slope. Figure 9(b) shows that coarse particles concentrate near the wall when they build up as is the case with the surge hopper.

Figure 11 shows changes in the mean size of particles discharged each time. The vertical axis is the mean particle size that has been normalized by the mean size of all the particles charged into the hopper. The graph shows that as time passes, the mean size of discharged particles increases. That is to say, this figure shows that particles smaller than the average are mainly charged in the ear-

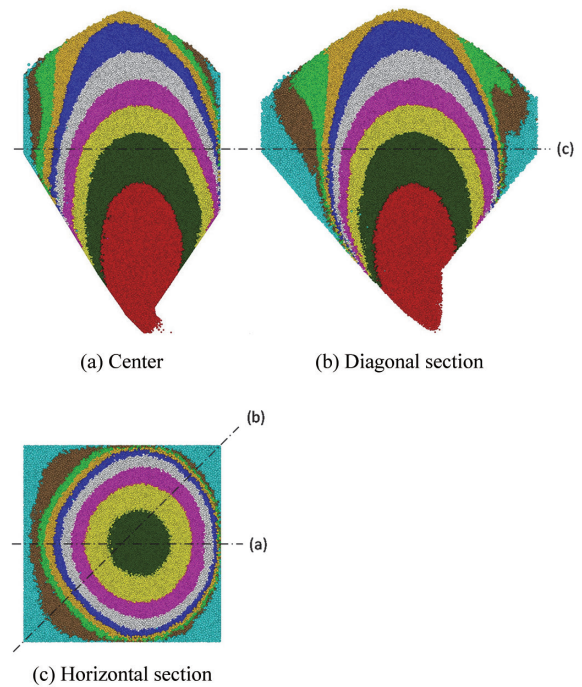


Fig. 7 Mapping of discharged timing from the surge hopper

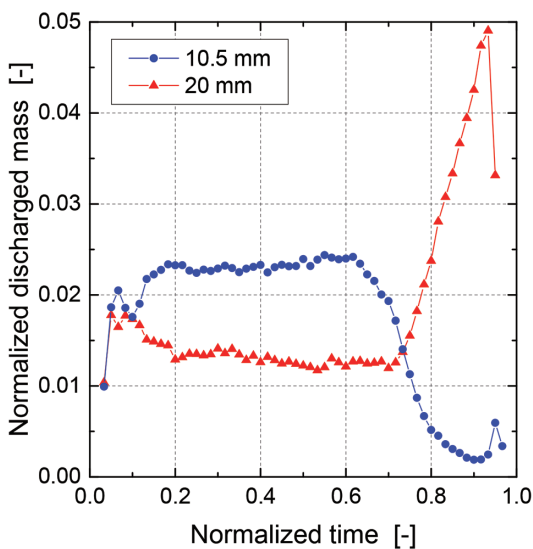


Fig. 6 Relation between the normalized discharge mass and the normalized time

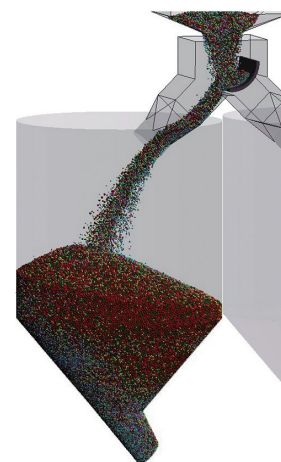


Fig. 8 Snapshot of particle behavior during charging into the parallel hopper (80 s)

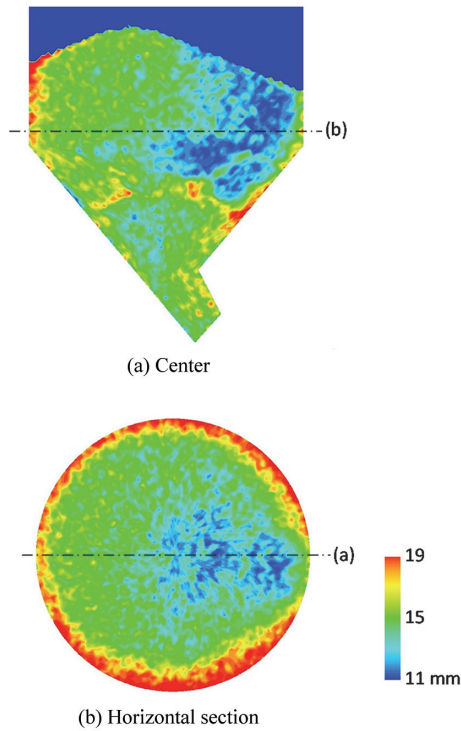


Fig. 9 Contour mapping of mean particle size of charged particle in the parallel hopper

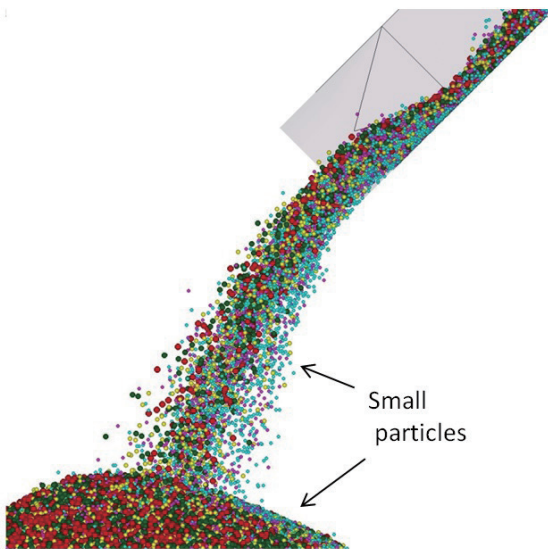


Fig. 10 Snapshot of particle discharging behavior at the outlet of transfer chute

ly stage of the charging into the furnace and after the normalized time of 0.7, particles larger than the average are charged. This trend is similar to the discharging from the surge hopper; particles in the center of the hopper are discharged in the early stage and the discharge of coarse particles building up near the wall lags, as shown by the discharge timing map of Fig. 12.

As explained above, the DEM simulation has reproduced the behavior that when sinter particles are charged into and discharged from the hoppers repeatedly during transportation to the blast fur-

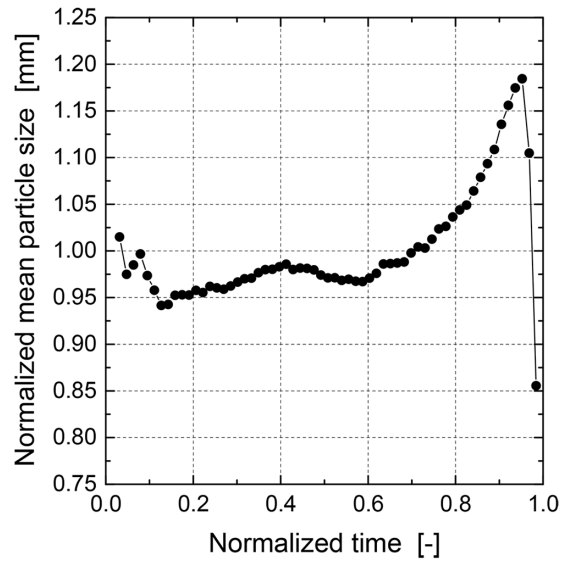


Fig. 11 Relation between the normalized mean particle size and the normalized time

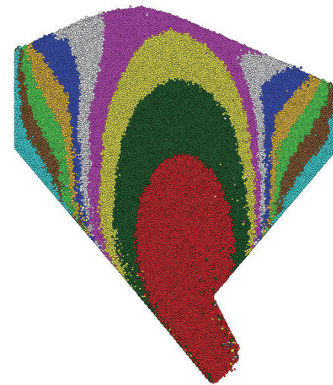


Fig. 12 Mapping of discharged timing in the parallel hopper

nace, they segregate; and in the latter period of the charging into the furnace, coarse particles gather. As a strong point of DEM, DEM can analyze in detail why such time-series changes occur and the conditions in a sedimentary layer, which is impossible to observe by experiments. DEM is a very useful simulation technique to study transportation procedures for controlling segregation, to study equipment design, and to optimize the distribution of particles charged into a furnace.

5. Conclusions

This paper introduced the analysis results of particle segregation during transportation in the process for charging particles into a blast furnace in the particle simulation using DEM. DEM that can analyze in detail the behavior of individual particles can obtain various information such as information on the inside of a sedimentary layer and time-series change, which is impossible to observe by experiments. Such information can be effectively used to clarify the mechanisms that control phenomena and to design operations and processes. This technique is expected to further advance in the future. However, many factors (e.g., shape of particles, surface properties, and water content) affect the behavior of particulates, so if the

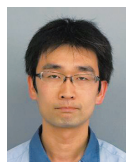
simulation has captured actual phenomena properly, it needs to be verified in detail by comparing the results to actual process phenomena. In addition, the computation speed needs to be significantly increased, so in the future, verification based on the phenomena seen in actual furnaces is required and large-scale computation algorithms on larger computers need to be developed.

References

- 1) Cundall, P.A., Strack, O.D.L.: *Geotechnique*. 29, 47 (1979)
- 2) Bertrand, F. et al.: *Chem. Eng. Sci.* 60, 2517 (2005)
- 3) Moreno, R. et al.: *Powder Technol.* 130, 132 (2003)
- 4) Rajamani, R. K. et al.: *Powder Technol.* 109, 105 (2000)
- 5) Cleary, P.W., Sawley, M.L.: *Appl. Math. Model.* 26, 89 (2002)
- 6) Ketterhagen, W.R. et al.: *Powder Technol.* 179, 126 (2008)
- 7) Taberlet, N. et al.: *Phys. Rev. E*. 73, 050301 (2006)
- 8) Kaneko, Y. et al.: *Chem. Eng. Sci.* 54, 5809 (1999)
- 9) Kawaguchi, T. et al.: *Powder Technol.* 109, 3 (2000)
- 10) Severens, I.E.M. et al.: *Granul. Matter.* 8, 137 (2006)
- 11) Yuu, S. et al.: *ISIJ Int.* 45, 1406 (2005)
- 12) Zhou, Z. et al.: *ISIJ Int.* 45, 1828 (2005)
- 13) Nouchi, T. et al.: *Tetsu-to-Hagané*. 92, 955 (2006)
- 14) Mio, H. et al.: *ISIJ Int.* 47, 1745 (2007)
- 15) Natsui, S. et al.: *ISIJ Int.* 51, 41 (2011)
- 16) Yu, Y., Saxén, H.: *ISIJ Int.* 52, 788 (2012)
- 17) Kim, S.Y., Sasaki, Y.: *ISIJ Int.* 53, 2028 (2013)
- 18) Mio, H. et al.: *ISIJ Int.* 48, 1696 (2008)
- 19) Mio, H. et al.: *ISIJ Int.* 49, 479 (2009)
- 20) Mio, H. et al.: *ISIJ Int.* 50, 1000 (2010)
- 21) Mio, H. et al.: *Miner. Eng.* 33, 27 (2012)
- 22) Mio, H. et al.: *ISIJ Int.* 57, 272 (2017)
- 23) Narita, Y. et al.: *ISIJ Int.* 57, 429 (2017)



Hiroshi MIO
Senior Researcher, Dr. (Eng.)
Ironmaking Research Lab.
Process Research Laboratories
20-1 Shintomi, Futtsu City, Chiba Pref. 293-8511



Yoichi NARITA
Researcher
Ironmaking Research Lab.
Process Research Laboratories